

Dynamic Performance Validation of High-Speed-Train-based on Finite Element Ear Model

Pengpeng XIE¹, YongPENG^{1,2}, Zhigang YANG¹

¹ *Key Laboratory of Traffic Safety on Track of Ministry of Education, School of Traffic & Transportation Engineering, Central South University, Changsha, 410075, China*

² *State Key Laboratory of High Performance Complex Manufacturing, Central South University, Changsha, 410006, China*
Email: yong_peng@csu.edu.cn

Abstract: The transient pressure changes generated by high-speed train's passing through tunnels inextricably causes discomfort of human ears, which goes more intensive with train's increasing velocity. To evaluate the discomfort levels and potential ear trauma from biomechanical aspects, a functional human ear model was established by micro-computer tomography. An adult volunteer with no records of hearing and respiratory injuries was initially selected for temporal bone CT scanning and the ear Finite Element (FE) model (Left ear) was developed based on the images data in Mimics, including auricle, ear canal, tympanic membrane(TM), ossicular chain, suspensory ligaments/tendons, incudomalleolar and incudostapedial joints. By structural-acoustic coupling and harmonic response simulation, the frequency responses of TM and stapes footplate were achieved, as well as sound pressure level (SPL) of stapes footplate derived from acoustic transfer function. The results indicate that the established human ear model has a good agreement with published experimental results, which means the human ear FE model was verified preferably for further research on high-speed train barotrauma of human ears.

Keywords:High-speed Train, Ear FE Model, Acoustic-structural Coupling, Harmonic Response

1 Introduction

Human ear is a complex acoustic-structural-liquid coupled system exposed to various atmospheric conditions. If the ambient pressure changes within human ears' allowing limits, an instant reaction and adjustment will be made by human ear. However, high-speed train's passing through tunnels or two meeting trains^[1-2], aircraft^[3], bomb blast^[4], diving^[5] are exceptions for reasons that subjects involved in these transportation tools or activities may frequently encounter sharp pressure changes far beyond the human ears' physiological responding ability. Until currently, abundant work has been done concerning train-tunnel effect. The nature of pressure gradient, compression and explosion wave was studied comprehensively covering train entry and intersection in tunnel scenarios^[6-9]. Even further, Lee et al.^[10] revealed the relationship between annoyance level and noise by virtue of hearing-healthy volunteers' participation in experiments and sound imaging technique. Despite these accomplished fruits, how pressure wave affects human ears comfort biophysically or ear barotrauma pathology caused by train-tunnel interaction hasn't been touched yet.

Thanks to the development of Computed Tomography (CT) and Magnetic Resonance Imaging (MRI), ears' anatomical structures can be observed and reconstructed in software. Since the first cat middle ear FE model was reconstructed^[11], diversified human ear model has been reported ranging from ear canal to inner ear through CT or MRI scanning. Especially, Gan carried out a leading series of middle ear researches reaching as far as ear reconstruction methods, middle ear sound transmission properties, acoustic-structural coupling numerical simulation, ear lesion and pressure distribution in ear canal and mastoid cavity^[12-16]. However, an intact auditory system from pinna to inner ear hasn't been accessible until recently. China's total railway mileage ranks the longest in the world accompanied with its tunnel coverage. Thus, it's meaningful to introduce ear barotrauma induced by train-tunnel effect into high-speed train and to tap into passenger noise comfort from biomechanics. In the paper, an intact human ear model was reconstructed through Mimics and reverse engineering and was warranted validity to go on with ear injury mechanism study by comparison with published data.

2 Method and Materia

2.1 Geometric model

Healthy volunteers (Male, average age: 25, left ear) with no history of hearing diseases are selected to take CT scanning (Siemens Somatom 16 slice spiral CT scanner was applied to collecting tomographic images) and acquired the fault images of each volunteer. It is noted that volunteer who has ever suffered with media otitis, rhinitis, middle ear operations or prosthetic experiences was excluded for a purpose of depending following ear injury research on a reliably undamaged ear. Import these CT images into Mimics and choose an appropriate view as the main reconstruction resource with the help of another two views, as shown in Fig.

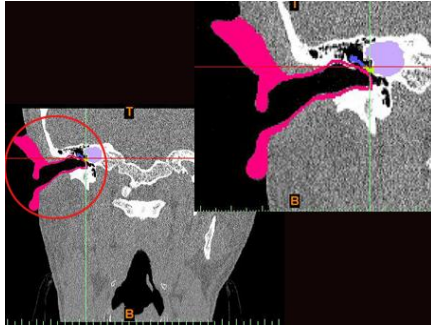
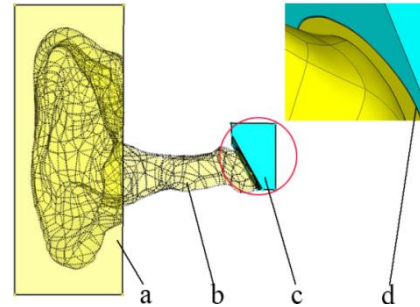


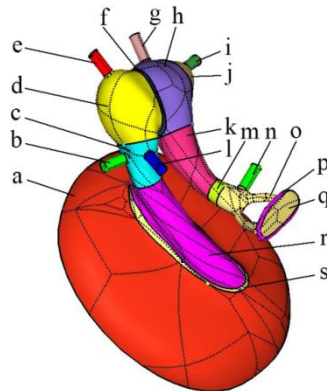
Fig.1 basic plane for reconstruction in coronal plane



a. outer ear domain b. ear canal domain c. mastoid cavity domain d. TM

Fig.2 air domain for acoustic FE analysis

While ear components marked with different colors are shaped, the model still exists with some invisible holes or cavities. Most importantly, the model derived from Mimics is comprised of triangle patches and isn't feasible for finite element analysis. Thus, Geomagic software and Hypermesh are utilized to build a smooth 3D ear model, as shown in Fig.2.



a. TM b. anterior malleal ligament c. malleus neck d. malleus head e. superior malleal ligament f. incudomalleolar joint g. superior incudal ligament h. incus body i. posterior incudal ligament j. short process k. long process l. lateral malleal ligament m. incudostapedial joint n. stapedial tendon o. stapes p. stapedial annular ligament q. stapes footplate r. malleus handle s. tympanic manubrium

Fig.3 structural domain for acoustic FE analysis

Some explanations should be made for the ear model. In Fig.1, the auricle and ear canal are eliminated except for middle ear considering that it is the displacement of ossicle chain that we care rather than that of auricle and ear canal wall which are extremely slight as well. Mastoid cavity, which is filled with air, is added for pressure balance and simplified in shape. Noticeably, there is a gap between ear canal and mastoid cavity where is the TM located. Though different TM thickness was reported^[16-18], the most commonly used is 0.05mm as is applied in this paper. A few cylinders were created as a replacement of middle ear ligaments. In addition, the middle ear model displayed in Fig.2 is sliced into plenty of components from one part for the convenience that the connection between attached components are nodes-shared.

2.2 FE model and materials

Middle ear model has complicated surfaces due to the varying curvature. Tetrahedral solid mesh is a good way to achieve a fine proximity to the real shape of middle ear. Moreover, TM is inclusively meshed by tetrahedral on account that shell element is not practical despite of a tiny thickness. On the other hand, shell element will cause TM's disconnection between ear canal air domain and mastoid cavity domain. For acoustic Finite Element Method (FEM), element size shouldn't exceed one sixth of the minimum sound wave length. In this paper, the analyzed frequency is low and mediate frequency band ranging from 200Hz to 10000Hz, corresponding with a minimum wave length of 0.57mm or so. Limited by the geometric size of ossicular bones and suspensory ligaments, mesh size as small as 0.05mm is favorable for improved element quality and 0.4mm for air domains instead. From clinical perspective, TM is bonded to ear canal skin at one side and mastoid cavity wall at the other side. One end of middle ear ligaments and tendon is attached to mastoid cavity wall while the other linked to ossicular bones. It should be distinguished that stapedial annular ligament is connected to oval window, which can be treated as fixed state while the stapes footplate it circled is movable like a piston. Thus, one entity set that added some of TM, ligaments and tendon's nodes was created to constraint the six freedom degrees, as shown in Fig.4.

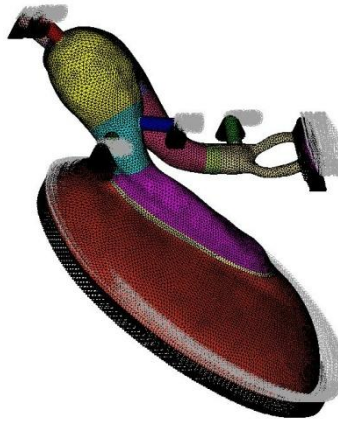


Fig.4 constrained middle ear FE model

Material definition is another concern that plays a role in modal analysis and harmonic response as a result of non-uniform ligament properties^[16-18]. Although different material properties are defined in previous papers, their middle ear models, whose dynamic responses were in consistency, were not the same too. Consequently, with regard to the FE model established in the paper, tetrahedral element type is likely to bring an exaggerated structural stiffness. Smaller ligament and tendon Young's module is liable to counteract some stiffness of the middle ear model, the detailed component properties are shown in Table.1.

2.3 Acoustic Boundary Conditions and Validation Methods

To validate the credibility of the FE ear model, the principal idea is to compare the simulation results with experimental data from cadaveric temporal bone test and healthy volunteer test. Volunteer test is to measure the healthy subjects' hearing sensibility to sound at certain frequency spectrum conducted by American National Standard Institute(ANSI) and a curve was plotted which denotes the minimum frequency-dependent SPL audible to human ears. Temporal bone test is to record the responses of stapes footplate via exerting an acoustic incentive of given SPL at TM. Correspondingly, two methods were employed to simulate the functionality of middle ear.

One is acoustic-structural coupling method and the other harmonic response analysis. The acoustic boundary conditions for the former method in details are: create a plane wave at a distance of 20mm from the aditus of ear canal to propagate pure tone sound and set the sound pressure from 2dB to 50dB with a step size of 2dB, the upper face, front face, two side faces and interfaces between middle ear and mastoid cavity are non-reflection boundary condition in accordance with the realistic condition, build two coupling faces for data transfer from ear canal to TM and middle ear to mastoid cavity, solve acoustic modes to confirm whether the acoustic boundary conditions are proper and structural modes for modal superposition to obtain dynamic response, solution frequency band is 200~10000Hz with a step size of 100Hz.

For harmonic response analysis, the cadaveric experiment is imposing a sound incentive of 90dB(0.63Pa) at the exterior of TM within 200~8000Hz, which is referred as initial simulation conditions too. In order to reduce the

calculation time, an entity set was created to select a couple of nodes as output points from umbilical region of TM and that of stapes footplate for observation where directly affect the sound pressure instead of computing the entire model.

Table1. Material properties of components of middle ear model

Component name	Density ρ 10^3kg/m^3	Young's Module E/Pa
TM	1.2	3.2E7
malleus	2.55(head)	1.41E10
	4.53(neck)	
	3.70(handle)	
incus	2.36(body)	1.41E10
	2.26(short process)	
stapes	5.08(long process)	1.41E10
incudomalleolar joint	2.2	1.41E10
incudostapedial joint	3.2	1.41E10
tympanic manubrium	1.2	6E5
anterior malleal ligament	1	4.7E9
lateral malleal ligament	2.5	2.1E6
superior malleal ligament	2.5	6.7E4
superior incudal ligament	2.5	4.9E4
posterior incudal ligament	2.5	4.9E4
stapedial annular ligament	2.5	6.5E5
stapes tendon	2.5	2E5
	2.5	5.2E5

3 Results and Discussion

3.1 Acoustic-structural coupling results

Acoustic modes analysis of outer ear domain offers an auxiliary way to check whether the acoustic boundary condition is appropriate, as shown in Fig.5.

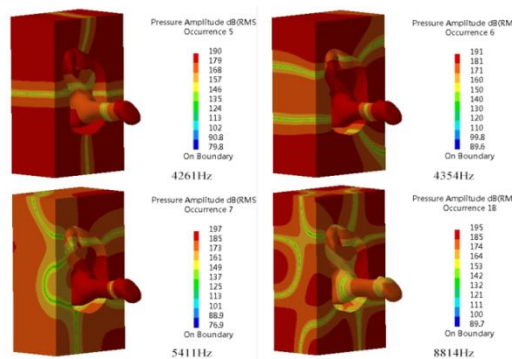


Fig.5 acoustic modes of outer ear domain at different orders

Sound wave interacts with head, pinna and ear canal when transmitting taking forms of scattering and diffraction. When the wave length is approximate to the ear size, resonance may happen. As is illustrated in Fig.4, at frequency of 4261Hz and 4353Hz, sound resonance appears at the pinna and head (the face that is close to middle ear is virtually regarded as part of head). With frequency increasing, the resonance area gradually transfers to ear canal. Assessing the

modal results, it implies that the mode patterns goes aligned with published data and coupling analysis is allowed to proceed.

The key process for human to feel sound is the movement of stapes footplate that stimulates the motion of the incompressible fluid within the oval window, by which the mechanical vibration is converted into electric signal to the brain. Inspired by this mechanism, the displacement of stapes footplate was choosed as an indicator to confirm sound has been detected. Through modal superposition acoustic-structural coupling method, dynamic responses of TM and stapes footplate were obtained as is shown in Fig.6.

From Fig.6, we observedthere existed slight displacement of stapes footplate in each picture and each picture corresponds with a given frequency value. For a visible comparison, two curves were plotted representing the minimum distinguishable sound pressure for human ear from ANSI experiment and simulation analysis respectively, as is shown in Fig.7

As is displayed in Fig.6, both curves present a sharp decline with increasing frequency and fluctuate slightly at 0.5~8kHz interval. Besides, the sound pressure will rebound steeply over 10kHz. For frequency-dependent human ear, it is the most sensitive to mediate frequency spectrum especially within a band from 1k to 4kHz. Most importantly, the simulation curve derived from vibro-acoustic coupling analysis keeps satisfactory agreement with ANSI experiment curve, which verifies the reliability of the constructed FE model in the paper.

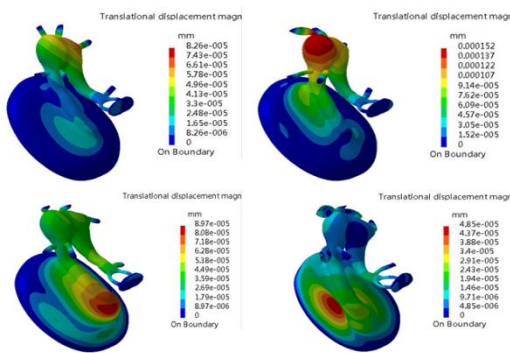


Fig.6 Displacement of TM and stapes footplate

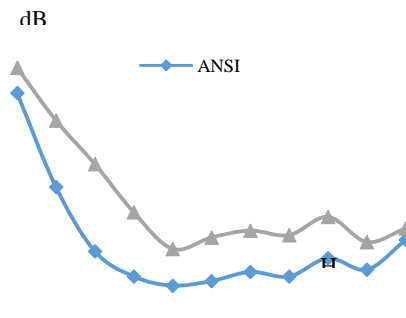


Fig.7 comparison between ANSI and simulation of human ear sensibility to sound

3.2 Harmonic response results

As is discussed previously, harmonic response analysis is to investigate the dynamics of middle ear without existence of acoustic domain. A 90dB(0.63Pa) pressure acted as sound excitation at the exterior of TM to drive the ossicular bones vibrating, the result is shown in Fig.8 to Fig.10.

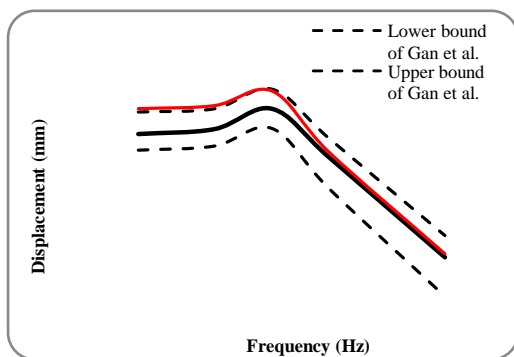


Fig.8 Comparison of TM displacement between FE model simulation and published measurements

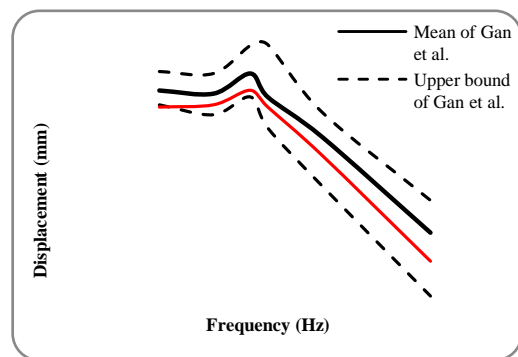


Fig.9 Comparison of Stapes footplate displacement between FE model simulation and published measurements

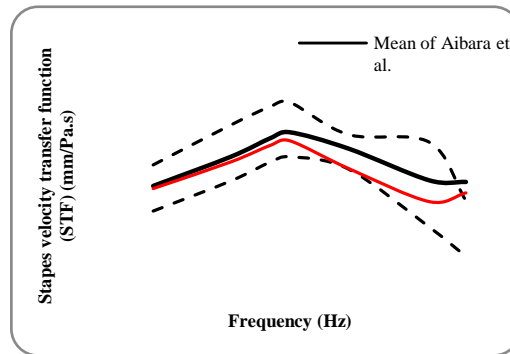


Fig.10 Comparison of STF between FE model simulation and published measurements^[19]

As is illustrated in Fig.8 and Fig.9, the dashed lines are originated from the measurement results of 14 fresh temporal bones response representing the two extremities of TM and stapes footplate displacement and the bold line is plotted by average values of tested specimens. From Fig.8, the FE model simulation curve is slightly higher than that of the upper bound line at frequency below 1kHz where peak magnitude is then it goes down closely to the mean curve but is significantly over the lower bound. However, in Fig.9 it is distinctly the opposite that the simulation line is constantly below the mean line and stays higher than lower bound line. Broadly, the result obtained from simulation doesn't go beyond the two bound lines but also has consistency with the experimental measurements meanwhile.

Similarly, the simulation curve is tightly adjacent to the mean line below 1kHz and separates at 1k~2kHz with a wider deviation. It isn't difficult to observe that the simulation line gets closer to the lower bound and the tendency of the four curves differs somewhere as a result of the individual discrepancy of human ears.

4 Conclusion

High-speed train offers preferable convenience for travelers in the wake of train-tunnel effect on human ear concerning comfort level and latent ear barotrauma. To make deep insight in ear annoyance and injury pathology, researchers have accomplished plentiful work from clinically and theoretically. It's conclusive that most investigators have established series of analogical FE ear models especially middle ear model. What should be emphasized is the FE ear model constructed in the paper is more intact on account of taking integrated consideration of pinna and ear canal and mastoid cavity which have sound collection functionality. We first recruited several healthy volunteers with no histological records of ear injury and obtained their temporal bone CT scanning images. As a follow, medical reconstruction and reverse engineering techniques were exploited to process the CT images in Mimics and a comparatively intact 3D ear model was created eventually consisting of auricle, ear canal, TM, ossicle bones and suspensory ligaments and tendons.

In sequence, we divided the model into acoustic domain and structural domain in need of vibro-acoustic coupling and harmonic analysis. Both methods, which are set the same boundary conditions with experiments, are to validate the reliability of the FE ear model by comparison with published results. In Fig.6 we found the most distinct reaction to sound is when the frequency band lies in 1k~8kHz for frequency-dependent human ear. Despite the fact the predicted sensibility curve derived from acoustic-structural coupling is higher than that from experiment, it is allowable because of individual discrepancy such as pinna size, ear diameter and length, middle ear structural differences. On the other hand, tetrahedral element type may stiffen the middle ear, which would result in decrease of footplate displacement. From Fig.7 to Fig.9, we realize that the displacements of TM and stapes footplate and simulation STF curve occur consecutively within the lower and upper area either higher or smaller than the mean line. When sound is transmitted into ear and stimulates the TM to vibrate, it is the first receptor which is undoubtedly deemed to generate a large displacement. As for stapes footplate, the movement may be weakened due to the damping effect of middle ear. That's why the simulation line in Fig.7 is superior to the mean line while the opposite in Fig.8.

To sum up, the FE ear model and acoustic-structural method are practicable to simulate the dynamic response of human ears. The model can contribute a fairly effective way to carry out researches on coupling effect of high-speed train noise and passengers comfort level and to predict potential barotrauma caused by transient pressure from perspective of injury biomechanics. In addition, the FE model is competent to study ear lesion pathology as well.

Acknowledgement

The research is supported financially by National Natural Science Foundation (No.5140051330) and China Postdoctoral Science Foundation (No.149882).

References

- [1] Chu C.R., Chien S.Y., Wang C.Y., et al. Numerical Simulation of Two Trains Intersecting in a Tunnel[J]. Tunnelling and Underground Space Technology, 2014, 42: 161-174.
- [2] Ko Y.Y., Che C.H. n, Hoe I.T., et al. Field Measurements of Aerodynamic Pressures in Tunnels Induced by High Speed Trains[J]. Journal of Wind Engineering and Industrial Aerodynamics, 2012, 100:19-29.
- [3] D. Aggromito, R. Thomson, J. Wang, et al. Effect of body-borne equipment on injury of military pilots and aircrew during a simulated helicopter crash[J]. International Journal of Industrial Ergonomics, 2015, 50:130-142
- [5] A.L. Dougherty, A.J. MacGregor, P.P. Han, et al. Blast-related Ear Injuries among U.S. Military Personnel[J]. Journal of Rehabilitation Research & Development, 2013,50(6):893-904
- [6] G.D. Becker, G.J. Parell. Barotrauma of the Ears and Sinuses after Scuba Diving[J]. Eur Arch Otorhinolaryngol, 2001, 258:159-163
- [7] P. Ricco, A. Baron, P. Molteni. Nature of pressure waves induced by a high-speed train travelling through a tunnel[J]. Journal of Wind Engineering and Industrial Aerodynamics, 2007,95:781-808
- [8] M. Rabani, A. K. Faghieh. Numerical analysis of airflow around a passenger train entering the tunnel[J]. Tunnelling and Underground Space Technology, 2015,45:203-213
- [9] D. Uystepuyst, M.W. Louis, E. Creuse, et al. Efficient 3D numerical prediction of the pressure wave generated by high-speed trains entering tunnels[J]. Computers & Fluids, 2011,47:165-177
- [10] D. Cross, B. Hughes, D. Ingham, et al. A validated numerical investigation of the effects of high blockage ratio and train and tunnel length upon underground railway aerodynamics[J]. Journal of Wind Engineering and Industrial Aerodynamics, 2015,146:195-206
- [11] P.J. Lee, J.Y. Hong, J.Y. Jeon. Assessment of rural soundscapes with high-speed train noise[J]. Science of the Total Environment, 2012,482-483:432-439
- [12] W.R. Funnell, S.M. Khanna, W.F. Decraemer. On the degree of rigidity of the manubrium in a finite element model of the cat eardrum[J]. J Acoust Soc Am, 1992,91(4):2082-2090
- [13] Sun Q.L., Chang K.H., Gan R.Z., et al. An advanced computer-aided geometric modeling and fabrication method for human middle ear[J]. Medical Engineering & Physics, 2002,24:595-606
- [14] Gan R.Z., Sun Q.L., Feng B., et al. Acoustic-structural coupled finite element analysis for sound transmission in human ear-Pressure distributions[J]. Medical Engineering & Physics, 2006,28:395-404
- [15] Gan R.Z., B.P. Reeves, Wang X.L.. Modeling of sound transmission from ear canal to cochlea[J]. Annals of Biomedical Engineering, 2007, 35(12):2180-2195
- [16] Gan R.Z.. Mechanical properties of stapedial tendon in human middle ear[J]. Journal of Biomechanical Engineering, 2007,129:913-918
- [17] Gan R.Z., Feng B., Sun Q.L.. Three-dimensional finite element modeling of human ear for sound transmission[J]. Annals of Biomedical Engineering, 2004,32(6):847-859
- [18] Lee C.F., Chen P.R., Chen W.J., et al. Three-dimensional reconstruction and modeling of middle ear biomechanics by high-resolution computed tomography and finite element analysis[J]. Laryngoscope, 2006,116(5):711-716
- [19] T. Koike, H. Wada, T. Kobayashi. Effect of depth of conical-shaped tympanic membrane on middle ear sound transmission[J]. JSME Int J, 2001,44:1097-1102
- [20] R. Aibara, J.T. Welsh, S. Puria, R.L. Goode. Human middle ear sound transfer and cochlear input impedance[J]. Hearing Res, 2001,152:100-109